ELSEVIER

Physica D 120 (1998) 255–272

PHYSICA D

The invariant density of a chaotic dynamical system with small noise

R. Kuske [a,*], G. Papanicolaou [b,1]

[a] *School of Mathematics, University of Minnesota, Minneapolis, MN 55455, USA*
[b] *Department of Mathematics, Stanford University, Stanford, CA 94305, USA*

Received 31 October 1997; received in revised form 9 February 1998; accepted 20 February 1998
Communicated by C.K.R.T. Jones

Abstract

We consider a chaotic dynamical system perturbed by noise and calculate an approximate invariant density when the noise level is small. Because of the special structure of the dynamical system, the effective support of the invariant density is much smaller than the noiseless attractor. This behavior is captured by the asymptotic form of the invariant density, which is given explicitly. © 1998 Elsevier Science B.V.

1. Introduction

We consider a dynamical system in which the effect of small noise on its chaotic behavior is described effectively by an invariant probability density that is concentrated around a closed curve in the invariant manifold of the system. The stochastic dynamical system has the form

$$d\mathbf{x} = \mathbf{U}(\mathbf{x})\,dt + \sqrt{2}\epsilon\sigma\,d\boldsymbol{W}, \tag{1.1}$$

and explicitly

$$dx = (\mu x - y^2 + 2z^2 - \delta z)\,dt, \quad dy = y(x-1)\,dt + \sqrt{2}\epsilon\,dW, \quad dz = (\mu z + \delta x - 2xz)\,dt, \tag{1.2}$$

where dW is white noise and ϵ is a small parameter that determines the noise level. This system was first considered in [1] as a model for chaotic effects in three-wave mode coupling. It was considered further in [2], where the very substantial effects of noise were analyzed.

In this paper we get an asymptotic expansion for small ϵ for the invariant probability density of the diffusion Markov process defined by (1.2). We use matched asymptotic expansions based on a Gaussian form for the density, constructed around an approximate periodic orbit of a reduced version of the dynamical system. This allows us to

* Corresponding author. Work partially supported by an NSF Mathematical Sciences Research Postdoctoral Fellowship and NSF grant DMS-9704589.
[1] Work partially supported by NSF grant DMS-9622854 and by AFOSR grant F49620-95-1-0315.

PII: S0167-2789(98)00085-2

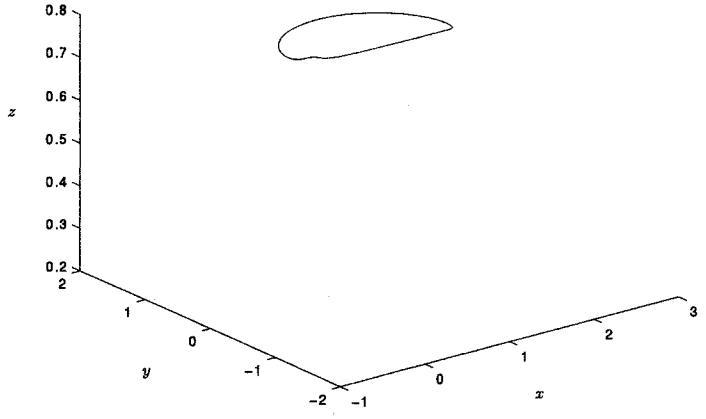

Fig. 1. Stable limit cycle for the deterministic system with $\delta = 1.5$ and $\mu = 0.01$. Note that this limit cycle is essentially on the plane $z = \delta/2$. Since the equations are invariant with change of sign in y, there is an identical limit cycle for $y > 0$.

assess quantitatively the effect of noise, which is to reduce substantially the size of the chaotic invariant manifold. The support of the invariant density includes all of the invariant manifold but most of its mass is concentrated on a small subset around an approximate periodic orbit, excluding the large excursions characteristic of chaotic behavior.

2. Qualitative description of the dynamics

The noiseless system, $\epsilon = 0$ in (1.2) is derived in [1] from a model of resonant wave mode interactions. The parameter $\mu \ll 1$ is the ratio of the small linear growth of one of the modes to the decay of the other two modes. This small parameter μ characterizes slow–fast dynamics, the significance of which is highlighted throughout the paper. The parameter $\epsilon \ll \mu \ll 1$ describes the strength of the noise and it must be small so as not to obscure completely the underlying dynamical behavior. However, it must not be too small (see (3.2)), as noted in [2], for the noise to have the important effects that we describe in this paper. The parameter δ is a linear combination of the wave numbers of the three wave modes, and is a bifurcation parameter.

The dynamical behavior of the noiseless system, (1.2) with $\epsilon = 0$, has been studied in [1], which we briefly summarize here. There are two fixed points, which are unstable for $\delta < 2$. For $\delta < 2$ but not too small, there is a stable limit cycle, as shown in Fig. 1. As δ decreases there is a sequence of period doubling bifurcations, leading to chaotic behavior for sufficiently small δ (see Fig. 2). The case $\delta = 0$ is singular, and we do not consider it here. However, we will discuss the case of $0 < \delta \ll 1$, for which the dynamical behavior is chaotic in the absence of noise.

In [2], Lythe and Proctor showed by a combination of analytical and numerical methods that for values of δ in the chaotic regime the presence of small noise has the effect of replacing the chaotic behavior with "noisy periodicity" (see Fig. 3). This means that noise reduces the size of the chaotic invariant manifold. More precisely, while the support of the invariant probability density of the noisy system includes all of the invariant manifold, most of its mass is concentrated on a small subset around an approximate periodic orbit.

In the work of [2] this phenomenon is explained in terms of the extreme values of x and their statistics. They showed that the large excursions in x are not present when small noise is introduced and the chaotic behavior is replaced by noisy periodicity.

We will now describe qualitatively the noisy global dynamics of the model (1.2). In the following sections we will get a detailed description of the invariant probability density that quantifies this behavior.

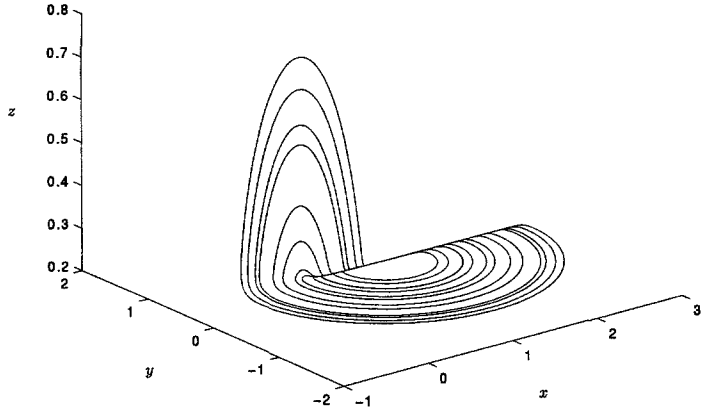

Fig. 2. Chaotic dynamics for the deterministic system with $\delta = 0.5$ and $\mu = 0.01$. Large excursions in z off the plane $z = \delta/2$ follow from large excursions in x. The variable y is initially negative here.

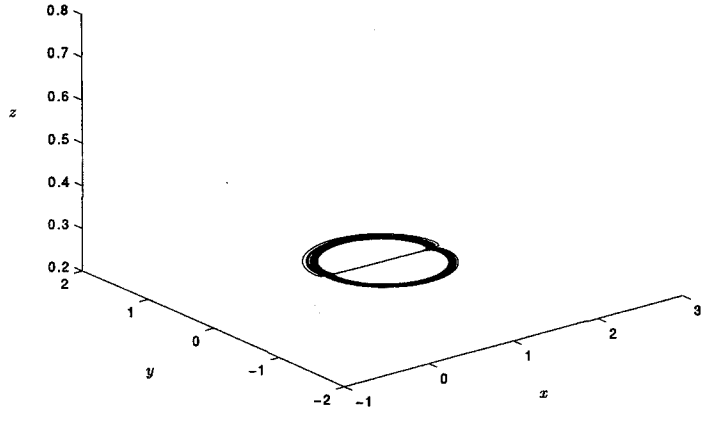

Fig. 3. Trajectory of the stochastic dynamical system with $\delta = 0.5$ $\mu = 0.01$ and $\epsilon = 10^{-7}$. Note that it stays close to the plane $z = \delta/2$ and looks like the orbit of Fig. 1, for both positive and negative y in a symmetric way. The chaotic character of the deterministic dynamics and the large excursions in x and z, shown in Fig. 2, are no longer present.

We note that noise is added to only one of the equations in (1.2). We could add small noise to the other equations as well but there would be very little change in the dynamics. This is because the bifurcations are organized about the approximate invariant line $y = 0$, $z = \delta/2$, when μ is small. That is, all trajectories, whether on a stable limit cycle or a chaotic orbit, approach $y = 0, z = \delta/2$ for $x \to 1$ with $x < 1$. The underlying slow–fast dynamics, characterized by μ being small, allow y to decay exponentially for $x < 1$ while x increases on the slow time scale μt. The closer the orbit gets to $y = 0$, the larger the excursion in the x and z variables at a later time. This can be seen by comparing Figs. 1 and 2. In Fig. 1, $\delta = 1.5$ and the orbits do not get very close to $y = 0$. In Fig. 2, $\delta = 0.5$ and the orbits get to within 10^{-20} of $y = 0$, which results in large x and z excursions. This aspect of the dynamics is described analytically by determining explicitly in the following sections the invariant probability density. Adding small noise to the y variable perturbs this exponentially (in $1/\mu$) close approach to the line $y = 0$, $z = \delta/2$ and in this way suppresses the large excursions of the x and z variables. This explains why adding noise to the y equation is the most interesting case. The presence of noise in only one equation requires that we check a hypoellipticity condition for the existence of a smooth invariant probability density, as we do in Appendix A.

3. Statement of results

The main result of this paper is the construction of an asymptotic expansion for the invariant probability density for the process defined by (1.2). The form of the invariant density gives an immediate description of the effect of the noise. We show, in particular, that the density is concentrated about a curve whose size is dictated by the magnitude of the noise and the slow–fast dynamics. The concentration of the invariant density about this curve varies considerably. The form of the density is

$$p(x, y) \sim K(x) \exp\{-(y - F(x) + \epsilon/\sqrt{g_n(x)})^2 g(x)/(2\epsilon^2)\}, \tag{3.1}$$

so that $y = F(x) - \epsilon/\sqrt{g_n(x)}$ describes the curve around which the distribution is centered, and $g(x)$ describes the variation of probability concentration about this center. The functions $F(x)$ and $g(x)$ are given explicitly in Appendix C. The function $F(x)$ comes from the deterministic dynamics, so that $F(x) - \epsilon/\sqrt{g_n(x)}$ represents the small perturbation to the deterministic behavior, unless $\epsilon g_n(x)$ is comparable to, or larger than, $F(x)$.

The density is given locally by three separate expansions, in the regions $y \ll 1$ and $|x - 1| = O(\mu)$, $y \ll 1$ and $|x - 1| = O(\mu^{1/2})$, and $y = O(1)$. In each of these regions, $F(x)$ and $g(x)$ are determined up to a constant, and the uniform result is obtained by matching the local expansions. Because the functions $F(x)$ include undetermined constants, the location of the center of the density is undetermined until the matching is performed. This matching yields a center for the density which is shown in Fig. 4. It is given by Eqs. (C.3), (C.8), and (C.12).

From the matching we conclude that the condition

$$\epsilon \gg e^{(C_1 - 1)/\mu} \equiv y_{\min}, \tag{3.2}$$

must be satisfied for the noise to have the dramatic effect of suppressing x and z excursions, as shown in [2]. In (3.2) $y_{\min}$ is the minimum of y for the noiseless dynamics. As shown in the matching in Appendix D, $y_{\min}$ can be related to $x_{\max}$, the maximum value of x on a trajectory. For example, in Fig. 2, $x_{\max} > 2$, so that $y_{\min} < 10^{-21}$. Similarly, we can conclude from (3.2) and the result of Appendix D that even when $x_{\max} = 2$ for the deterministic

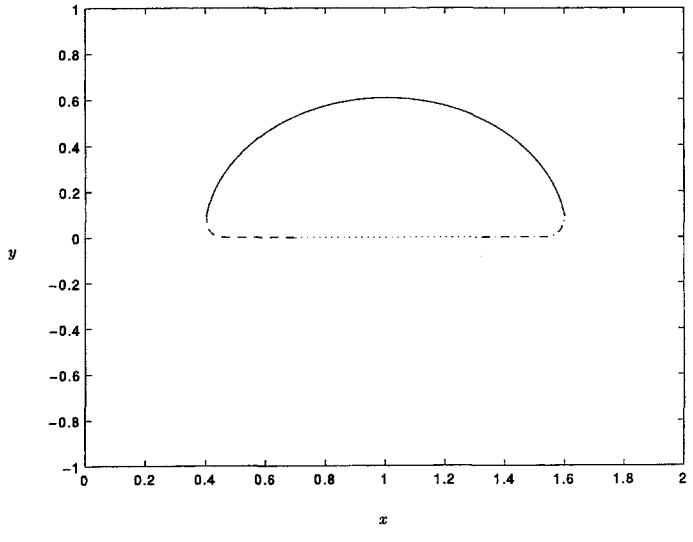

Fig. 4. The curve of maximum probability of the invariant density for $\mu = 0.01$ and $\epsilon = 10^{-7}$, as predicted by the analysis in Section 7 and Appendices C and D. This curve is constructed by matching the exponents of the Gaussian in the local expansions from Region 1 (dotted line), Region 2 (dashed and dashed–dotted lines), and Region 3 (solid line). Reflection across the x-axis gives the curve of maximum probability for negative values of y.

system, noise with magnitude as small as $\epsilon = 10^{-10}$ will have a significant effect. The matching also provides the maximum value of x for the noisy system,

$$(x_{\max} - 1)^2 = \mu(1 - 2\log\epsilon), \tag{3.3}$$

which fixes the location of the curve around which the invariant density is concentrated.

The matching of the functions $g(x)$, which describe the variation in concentration of the density, implies that for $y \ll 1$ and $|x - 1| = O(\mu)$, $g(x) = O(1)$, so that the width of the density is $O(\epsilon)$. However, for $y = O(1)$, $g(x) = O(\epsilon^2/\mu)$, so that the width of the density is $O(\mu^{1/2})$. In the intermediate region, $g(x)$ varies from $O(1)$ to $O(\epsilon^2/\mu)$, as shown in Appendix D. This transition in the width of the density is apparent from Figs. 5 and 6.

4. Numerical error in simulations of chaotic dynamical systems

Understanding the global dynamical behavior of (1.2) in terms of the relative sizes of its parameters and the noise yields some useful insight into its numerical simulation. For example, if noise with magnitude $\epsilon = 10^{-10}$ influences the dynamics, then care must be taken in controlling numerical error, even when solving the deterministic system. Fig. 7 shows the solution of (1.2) when this error is not properly monitored. Although the solution looks qualitatively correct, it can be easily deduced from (1.2) that there should be no crossings of $y = 0$, as happens in Fig. 7. Knowledge of where the error plays a significant role, that is, when the process is near the invariant line $y = 0, z = \delta/2$, suggests a simple way to avoid this numerical error, which cannot be done by naively reducing the time step. We must perform a "local" computation for very small values of y as follows. When y is sufficiently small, it can be rescaled to $y = \alpha\tilde{y}$ for $\alpha \ll 1$. Substituting in (1.2) yields

$$\dot{x} = \mu x - \alpha\tilde{y}^2 + 2z^2 + \delta z, \quad \dot{\tilde{y}} = \tilde{y}(x - 1), \quad \dot{z} = \mu z + \delta x - 2xz. \tag{4.1}$$

Thus the errors (which depend on machine precision) have been shifted into the equation for x, where they play no significant role in changing the large scale behavior of the system.

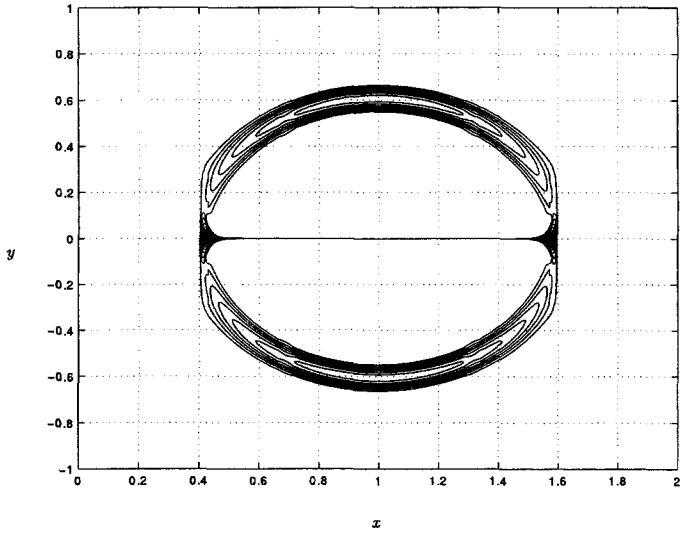

Fig. 5. Overlay of contour plots for $p_1(x, y)$, $p_2(x, y)$, and $p_3(x, y)$ for Regions 1, 2, and 3, respectively, as constructed in Section 7. The density $p_1(x, y)$ is sharply peaked for $y \ll 1$, while the wider spread of $p_3(x, y)$ describes the larger variation for $y = O(1)$. This behavior agrees with the simulations in Fig. 3 when projected onto the plane $z = \delta/2$ as shown in Fig. 6. Here $\mu = 0.01$ and $\epsilon = 10^{-7}$.

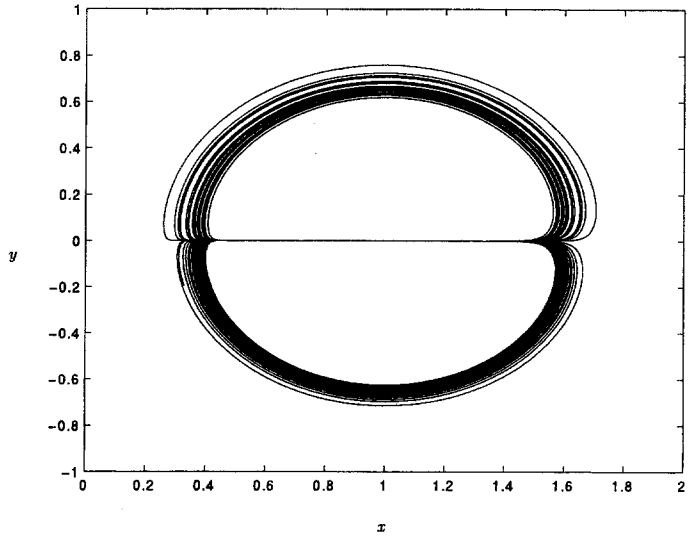

Fig. 6. The trajectory of the stochastic dynamical system of Fig. 3 when projected onto the plane $z = \delta/2$. Here $\mu = 0.01$ and $\epsilon = 10^{-7}$.

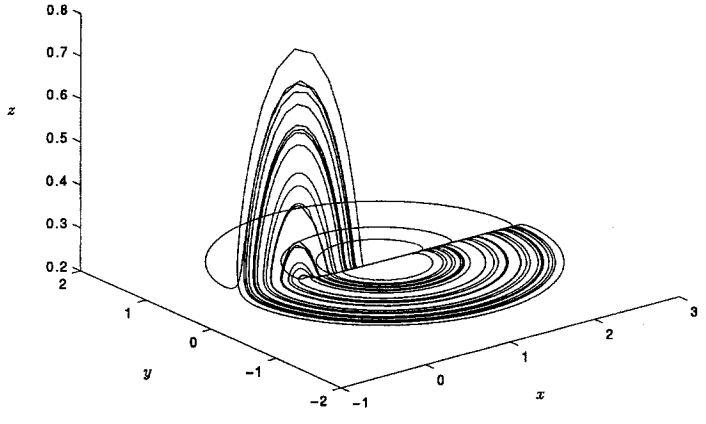

Fig. 7. Effect of numerical noise on the computation, for Δt small. The computations predict the correct qualitative behavior, but are quantitatively in error. The analysis predicts the size of computational error which is significant.

Computational issues in dynamical systems with random perturbations are considered in detail by Kifer [3].

5. Remarks about the analysis of noisy dynamical systems

There is an extensive literature on random dynamical systems with one or more stable equilibrium points or a limit cycle in which noise is added [4,5]. For problems in which noise causes transitions between stable equilibria, as in chemical kinetics [6], it is well known that the density can be approximated by a Gaussian in which the variance is expressed in terms of the ratio of the attracting force to the noise level. In [7] probability densities are constructed for some problems with stable limit cycles. In these problems the noise acts against the forces of attraction to the equilibrium points, or limit cycles, and can cause transitions between them.

Local Gaussian approximations are used in these problems, and elsewhere [5], as is done here. These local approximations give the location and the covariance of the Gaussian. The relative mass around each equilibrium is globally determined by variational methods or matching [5]. In this paper, we construct an approximation based on Gaussians in which the location and spatial variation of the width of the density are not specified until the matching is completed. Not knowing in advance the manifold (curve) around which the Gaussian is concentrated, is a consequence of the chaotic nature of the underlying attractor. Since there is no stable limit cycle, it is the noise that selects the region of concentration of the invariant density, within the chaotic attractor of the deterministic system. The excursions in x and z that characterize chaotic behavior of the deterministic system (Fig. 2) are still seen, on a limited scale, in the variation of the width of the invariant probability density.

The approximation of the invariant probability density by local Gaussians that fit together through matching can be viewed as solving approximately the stochastic Hamilton–Jacobi equation that comes from a WKB ansatz. This means that the invariant density has the form $p = e^{S/\epsilon^2}$ and the equilibrium equation $\mathcal{L}^* p = 0$ transforms into

$$\epsilon^2 S_{yy} + S_y^2 - \mathbf{U} \cdot \nabla S - \epsilon^2 \nabla \cdot \mathbf{U} = 0, \tag{5.1}$$

where $\mathbf{U}$ is the deterministic vector field of the dynamical system (1.1), (1.2). In Appendix C we, in effect, solve this equation approximately with suitable quadratic functions near the invariant manifold. The matching in Appendix D determines the manifold and the form of the density around it. In addition to the determination of the noisy behavior of the maximum excursion of the x variable, analyzed by Lythe and Proctor [2], our analysis gives a global description of the long-time statistical behavior of the trajectories.

The dynamical behavior of (1.2) may appear, at first glance, to be similar to that of the Lorentz system in [8,9]. In this model Lorentz system the bifurcations are organized about the unstable fixed point at the origin and a Lyapunov function is used to show that all orbits tend to a bounded set of zero volume [10]. It has further been shown by Bunimovich and Sinai [11,12] that there is a unique invariant measure on the deterministic attractor. In [8], it is shown that the invariant measure for the noisy Lorenz model converges weakly in the limit of zero noise to the deterministic one. The deterministic invariant measure was shown in [11,12] to be absolutely continuous with respect to Lebesgue measure generated by the length of smooth curves on the attractor.

In the dynamical system (1.2), it is not the fixed points which play a major role, but rather the approximate invariant line $y = 0, z = \delta/2$. This makes it difficult to extend the analysis of the Lorenz system and it may in fact be impossible to do this. Even if we had shown, as in the Lorenz system, that there is an invariant measure on the attractor to which the equilibrium probability law of the noisy system converges as the noise goes to zero, we would still not have had any information about the main result of this paper. That is, we would not have been able to explain analytically the suppression of x and z excursions by the noise and the concentration of the invariant probability on a curve in the (x, y) plane, as can be seen from Figs. 5 and 6. This effect is seen only when there is at least an exponentially small amount of noise (Section 3) and it disappears in the limit $\epsilon \to 0$.

6. Simplification of the invariant density equation

In this section we consider the equations for the invariant density for the process defined by (1.2). Since (1.2) is a system of stochastic differential equations, the time dependent probability density

$$p(t, x, y, z) \equiv \Pr(x(t) = x, y(t) = y, z(t) = z) \tag{6.1}$$

satisfies the Fokker–Planck equation (FPE)

$$p_t = \epsilon^2 p_{yy} - ((\mu x - y^2 + 2z^2 - \delta z)p)_x - (y(x-1)p)_y - ((\mu z + \delta x - 2xz)p)_z \equiv \mathcal{L}^* p. \tag{6.2}$$

The invariant probability density p (assuming it exists) is given by the stationary solution of this equation, which is $\mathcal{L}^* p = 0$. The uniqueness and regularity of the solution of (6.2) are insured by the hypoellipticity of the operator $\mathcal{L}^*$. This is a nondegeneracy condition on $\mathcal{L}^*$, as defined in [13] and is shown to hold in Appendix A. It is also necessary to show that the trajectories remain bounded with high probability. This is addressed in Appendix B. The remainder of this paper is devoted to approximating the invariant density $p(x, y, z)$ when ϵ is small. A general discussion of existence and uniqueness of invariant measures is given in [4].

We point out two special features of this problem before proceeding. There is a difficulty in determining the invariant measure, which comes from the form of the noiseless dynamics of (1.2). As described in [1], the trajectories spend a long time near the approximate invariant line ($y = 0$, $z = \delta/2$), rather than approximate fixed points. This requires an analysis of $\mathcal{L}^* p = 0$ which differs from the approach used for systems with stable fixed points, as in [14] or [6]. However, the special, degenerate structure of the operator $\mathcal{L}^*$ allows us to obtain an explicit analytical expression for the density, as shown below.

We first reduce the equation to a simpler one in two variables. As suggested by the dynamics and the simulations, the invariant density is concentrated near the plane $z = \delta/2$, and $y = 0$ for certain values of the parameters μ and δ. For the portion of the density concentrated near $z = \delta/2$ we introduce the change of variables

$$z = \frac{\delta}{2} + \mu\frac{\delta}{4x} + \zeta, \tag{6.3}$$

and obtain the system

$$\begin{aligned} \mathrm{d}x &= \left[\mu x - y^2 + \left(\frac{\delta}{2} + \mu\frac{\delta}{4x} + \zeta\right)\left(\frac{2\mu\delta}{4x} + 2\zeta\right)\right]\mathrm{d}t, \\ \mathrm{d}y &= (y(x-1))\,\mathrm{d}t + \sqrt{2}\epsilon\,\mathrm{d}W, \\ \mathrm{d}\zeta &= (\mu\zeta - 2x\zeta)\,\mathrm{d}t - \frac{\mu\delta}{4}\left[-\frac{\mu}{x} + \frac{\mu x - y^2}{x^2} + \left(\frac{\delta}{2} + \mu\frac{\delta}{4x} + \zeta\right)\left(\frac{2\mu\delta}{4x} + 2\zeta\right)\Big/ x^2\right]\mathrm{d}t. \end{aligned} \tag{6.4}$$

For $x > 0$ and $\mu \ll 1$, ζ decays exponentially. Therefore, in this region we assume that ζ is small and that the leading order dynamics is given by

$$\begin{aligned} &\mathrm{d}x \sim [\mu G(x) - y^2]\,\mathrm{d}t, \quad G(x) \equiv x + \frac{\delta^2}{4x}, \\ &\mathrm{d}y \sim y(x-1)\,\mathrm{d}t + \sqrt{2}\epsilon\,\mathrm{d}W, \end{aligned} \tag{6.5}$$

with ζ slaved to x as

$$\mathrm{d}\zeta \sim \mu\zeta - 2x\zeta\,\mathrm{d}t. \tag{6.6}$$

For the reduced system, the invariant density $P(x, y, \zeta)$ satisfies the equation

$$\epsilon^2 P_{yy} - ((\mu G(x) - y^2)P)_x - (y(x-1)P)_y - ((\mu\zeta - 2x\zeta)P)_\zeta = 0. \tag{6.7}$$

The small ϵ analysis can be simplified further by looking for leading order solutions of the form

$$P(x, y, \zeta) = q_1(x, y)q_2(x, \zeta), \tag{6.8}$$

with $q_1(x, y)$ satisfying

$$\epsilon^2 q_{1yy} - \left(\left(\mu x + \mu\frac{\delta^2}{4x} - y^2\right)q_1\right)_x - (y(x-1)q_1)_y \sim 0. \tag{6.9}$$

Once $q_1(x, y)$ has been computed, it is straightforward to substitute (6.8) in (6.7) and show that to leading order, $q_2(x, \eta) \sim \mathrm{e}^{-h(x)\zeta^2}$, with $h(x) > 0$ and $h(x) = \mathrm{O}(1)$ for $x > 0$. In the following we show that $q_1(x, y)$ is

concentrated on positive values of x for values of δ in the chaotic regime and is exponentially small for $x \ll 1$ and for $x < 0$. Then the behavior of $q_2(x, \zeta)$ indicates that the density is concentrated near $\zeta = 0$, that is, $z \sim \delta/2$. The main difficulty is determining $q_1(x, y)$ on which we focus the analysis of the following sections.

We give a brief demonstration of determining $q_2(x, \zeta)$. We show in Appendix C that $q_1(x, y)$ is negligible except in a neighborhood about a curve $y = F(x) - \epsilon/\sqrt{g_n(x)}$. Substituting this expression for y and (6.8) into (6.7) yields the equation for q_2,

$$(\mu G(x) - [F(x) - \epsilon/g_n(x)]^2)q_{2x} - (\mu\zeta - 2x\zeta)q_{2\zeta} - (\mu - 2x)q_2 \sim 0. \tag{6.10}$$

In Appendices C and D the functions $F(x)$ and $g_n(x)$ are determined by matching local expansions for $p_1(x, y)$ in three different regions. We demonstrate the solution of $q_2(x, \zeta)$ for Region 1, with $y \ll 1$ and $(x - 1) \ll \mu^{1/2}$. In this case $y \ll \mu$, and thus it can be neglected in (6.10). Then with the ansatz $q_2 = \sqrt{h(x)}e^{-h(x)\zeta^2}$ we find from (6.10) that

$$h = \exp \int \frac{4x - 2\mu}{\mu G(x)}\, dx. \tag{6.11}$$

Then $h(x)$ is exponentially large for small μ, so that $q_2(x, \zeta)$ is negligible except for $\zeta \sim 0$. Determining $q_2(x, \zeta)$ in the other regions is accomplished in the same manner.

7. The form of the expansion

We outline the procedure for obtaining an asymptotic approximation for the function $q_1(x, y)$. We may consider q_1 as the invariant density of a two-dimensional system of the form

$$dx = f_1\, dt, \qquad dy = f_2\, dt + \sqrt{2}\epsilon\, dW. \tag{7.1}$$

We use this in the following sections.

The Fokker–Planck equation for the invariant density $p(x, y)$ corresponding to the process (7.1) is

$$\epsilon^2 p_{yy} - (f_1(x, y, \mu)p)_x - (f_2(x, y, \mu)p)_y \equiv \mathcal{L}^* p = 0. \tag{7.2}$$

For $\epsilon = 0$, the trajectories are curves following $y = F(x, \mu)$. We use the change of variables

$$y - F(x, \mu) = \epsilon\zeta, \tag{7.3}$$

so that the equation $\mathcal{L}^* p = 0$ becomes

$$p_{\zeta\zeta} - \left(\frac{\partial}{\partial x} - \frac{F'(x, \mu)}{\epsilon}\frac{\partial}{\partial \zeta}\right)[f_1(x, F(x) + \epsilon\zeta, \mu)p] - \frac{1}{\epsilon}\frac{\partial}{\partial \zeta}[f_2(x, F(x) + \epsilon\zeta, \mu)p] = 0. \tag{7.4}$$

The $O(\epsilon^{-1})$ terms cancel, since $F'(x, \mu) = f_2(x, F(x), \mu)/f_1(x, F(x), \mu)$. Expanding about $\epsilon = 0$ yields the leading order equation,

$$\begin{aligned} &p_{\zeta\zeta} - f_1(x, F(x), \mu)\frac{\partial p}{\partial x} + \zeta f_1^{(2)}(x, F(x), \mu)F'(x, \mu)\frac{\partial p}{\partial \zeta} \\ &\quad - \zeta f_2^{(2)}(x, F(x), \mu)\frac{\partial p}{\partial \zeta} - f_1^{(1)}(x, F(x), \mu)p - f_2^{(2)}(x, F(x), \mu)p \sim O(\epsilon). \end{aligned} \tag{7.5}$$

Here $f_j^{(1)}$ and $f_j^{(2)}$ refer to differentiation of f_j with respect to x and y, respectively. Neglecting $O(\epsilon)$ terms, and (possibly) expanding about $\mu \ll 1$, we find that (7.5) suggests a solution of the form

$$\exp\{-\zeta^2 g(x) + \zeta q(x) + h(x)\}, \tag{7.6}$$

which can be written in terms of the original variables as

$$p(x, y) \sim K(x) \exp\{-(y - F(x) + \epsilon/\sqrt{g_n(x)})^2 g(x)/(2\epsilon^2)\}, \tag{7.7}$$

where

$$\begin{aligned} g_n(x) &= \exp\left(-2\int^x \frac{f_1^{(2)}F' - f_2^{(2)}}{f_1}\,dx'\right), \qquad g_d(x) = 2\int^x \frac{g_n(x')}{f_1(x')}\,dx', \qquad g(x) = \frac{g_n}{g_d}, \\ K(x) &= K_0 \exp\left(-\int^x \frac{f_1^{(2)}F' + f_2^{(2)}}{f_1}\,dx'\right)\Big/\sqrt{g_d}. \end{aligned} \tag{7.8}$$

We now discuss the nature of this approximation. The form of the density is readily interpreted in terms of the dynamics of the underlying process. It is clear that $p(x, y)$ is strongly peaked about $y = F(x)$, unless $\epsilon/\sqrt{g_n(x)}$ is comparable to $F(x)$. That is, whether the trajectories stay close to the deterministic ones depends on the relative size of $F(x)$ and $\epsilon/\sqrt{g_n}$. The "width" of the density is given by $2\epsilon^2/g(x)$. Qualitatively, if $g(x) \gg \epsilon^2$, the density is sharply peaked about $y = F(x) - \epsilon/\sqrt{g_n}$. If $g(x) \sim \epsilon^2$, then there is a larger variation about $y = F(x) + \epsilon/g_n$. We limit the expansion to quadratic terms in the exponent, Gaussians near the approximate invariant curve, as is usual in small noise approximations.

8. Three-dimensional effects

Certain characteristics of this model, such as large excursions of the chaotic trajectories, contraction and dilation of the attractor, slow–fast dynamics, and sensitivity to small noise have been observed in other models as described in [17].

We now explain briefly the generalization of our analysis to higher-dimensional problems. As demonstrated in Section 6, the density $p(x, y, z)$ is concentrated near the plane $z = \delta/2$, and for values of $x > 0$. For values of ϵ and δ used in the simulations, the variations of z away from $\delta/2$ are $O(\mu)$, even for very small values of ϵ and δ, as shown in Fig. 8. Therefore one could use the construction of Section 6 to determine the asymptotic behavior of the density. For purposes of illustration, we consider (1.2) for very small values of δ and ϵ, and show how a more detailed analysis of the density could be used to consider variations away from $z = \delta/2$ when $x \ll 1$ and $y \ll 1$.

We can generalize the expansion of the previous sections to show that the local approximations of the density have the form

$$p_4(\zeta, \eta, z) \sim \exp\{-\zeta^2 g(z)/2 + q(z)\zeta + h(z) - \frac{r^2}{2}\alpha(z) + r\zeta\beta(z) + r\gamma(z)\} \quad \text{for } x \ll 1,\ y \ll 1. \tag{8.1}$$

Here $\epsilon\zeta = \eta - F(z)$, $\epsilon r = \eta - H(z)$, $y = \mu^{1/2}\eta$, and $F(z)$ and $H(z)$ approximate the deterministic dynamics for $y \ll 1$ and $\mu \ll 1$,

$$x^2 = C_4 - z^2 = H^2(z), \tag{8.2}$$

$$\eta = \frac{1}{\sqrt{\delta/2 - z}} \exp\left[-\frac{1}{2}\int \frac{1}{\sqrt{C_4 - z^2}(\delta/2 - z)}\right]. \tag{8.3}$$

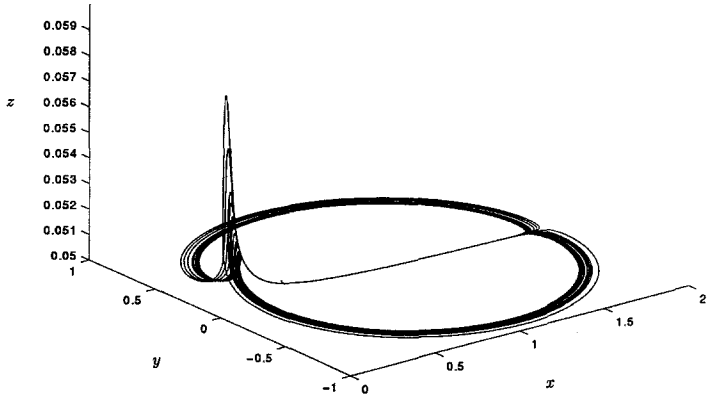

Fig. 8. For $\delta = 0.1$ and $\epsilon = 10^{-10}$ some variation away from the plane $z = \delta/2$ can be observed for the trajectories of the stochastic system. When the variations are sufficiently large the plane approximation of Section 7 cannot be used and z excursions must be taken into consideration as described in Section 8.

In this example it is not possible to obtain closed form expressions for the functions $g(z)$, $q(z)$ $h(z)$ $\alpha(z)$, $\beta(z)$ and $\gamma(z)$. They satisfy a system of coupled ordinary differential equations, which can be obtained by substituting p_4 into the appropriate reduced Fokker–Planck equation. In general, this system of equations must be solved numerically, as is done for a similar system in [18]. As in Appendix D, the matching of $p_4(x, y)$ with $q_1(x, y)q_2(x, z)$ determines the undetermined constant C_4, which describes the maximum variation of z from $\delta/2$ on the curve about which the density is concentrated. As discussed in Appendix B, $C_4 \sim x_{\min}^2 + \delta^2/4$, up to $O(\mu \ln \mu)$ corrections. Thus through this matching, it can be shown that the maximum variation in $z - \delta/2$ depends on the maximum value of x and the corresponding curve determined in Appendix D by matching the local expansions for $q_1(x, y)$. That is, larger excursions in x and y gotten from $q_1(x, y)$ translate into larger variations in $z - \delta/2$, captured by p_4 in (8.1).

9. Summary and conclusions

The main result of this paper is the construction of an asymptotic expansion for the invariant probability density for the process defined by (1.2). For small δ, μ and ϵ, this is a chaotic dynamical system with small noise. The form of the invariant probability density for small noise (3.1) gives a clear analytical description of the main effect of noise on the chaotic attractor, which is the suppression of the large, deterministic x and z excursions, as can be seen in Figs. 2 and 3. The location on the trajectories where noise effects are important can also be seen from the form of the invariant density, near the line $y = 0$, $z = \delta/2$. The matching of three local expansions for the density gives a quantitative description of these effects, as shown in detail in Appendices C and D. In particular, the condition (3.2) for the noise to have a significant effect, the location of the center and the width of the invariant density are found by matching the exponents in all regions, as explained in Appendix D.

The method that we have used for constructing an approximation to the invariant probability density, by matching of local Gaussian expansions, is quite general but not easy to implement in complicated dynamical systems with chaotic behavior. It is particularly useful in describing probability densities which have large variations in concentration. It has been applied recently to the description of probability densities for noisy systems in which the bifurcation parameter is slowly increased through a steady, or Hopf, bifurcation point, above which the basic state is unstable [18]. Without the noise, there is a delay in the transition from the basic state to the stable state and there is a reduction in the delay of the bifurcation when noise is added. The corresponding probability density function

is sharply peaked before the transition, and has an order of magnitude change in the spread in the region where the transition occurs. This is because of the variability of the transition caused by the noise.

The asymptotic expansion of the probability density can, moreover, be used to improve the efficiency of numerical solutions of the Fokker–Planck equation for the invariant density. Since the diffusion coefficient in the Fokker–Planck equation (6.2) is small, a straightforward grid-based method introduces numerical diffusion greater than the actual diffusion. Expansion (3.1) suggests how to place an adaptive grid for the computation of the density. Another class of numerical methods that can be used for convection-dominated convection–diffusion equations, such as (A.2), is (gradient) particle methods. If particle methods are used, expansion (3.1) provides an initial distribution of particles for faster convergence. These methods have been used to compute time-dependent probability densities for noisy delay bifurcations [18].

Appendix A. Hypoellipticity

We consider stochastic differential equations of the form

$$\mathrm{d}x = f_1(x, y, z)\,\mathrm{d}t, \qquad \mathrm{d}y = f_2(x, y, z)\,\mathrm{d}t + \sqrt{2\epsilon}\,\mathrm{d}W, \qquad \mathrm{d}z = f_3(x, y, z)\,\mathrm{d}t. \tag{A.1}$$

The transition probability density $p(t, x, y, z)$ satisfies the Fokker–Planck equation

$$\epsilon^2 p_{yy} - (f_1 p)_x - (f_2 p)_y - (f_3 p)_z \equiv \mathcal{L}^* p = p_t. \tag{A.2}$$

To show that the transition density exists and is a smooth function we consider the operators

$$L_2 = \epsilon\frac{\partial}{\partial y}, \qquad L_0 = \epsilon f_1\frac{\partial}{\partial x} + \epsilon f_2\frac{\partial}{\partial y} + \epsilon f_3\frac{\partial}{\partial z}, \tag{A.3}$$

and define the sets of operators

$$\begin{aligned} S_0 &= \{L_2, L_0\},\\ S_1 &= \{L_1 \equiv [L_2, L_0]\},\\ S_2 &= \{L_3 \equiv [L_0, L_1],\ L_4 \equiv [L_2, L_1]\},\\ &\vdots\\ S_m &= \{[L_j, L_k],\ L_j \in S_{m-1}, k = 0, 2\}, \end{aligned} \tag{A.4}$$

where the brackets denote commutators. We also define $\Sigma_M = \bigcup_{m=1}^{M} S_m$. Then, for each (x, y, z) if there exists an M such that there are $d = 3$ operators in Σ_M that are linearly independent, the transition density p, solution of (A.2), is smooth. This is a nondegeneracy condition on the operator $\mathcal{L}^*$ (hypoellipticity) [13].

We demonstrate this for the stochastic equations (1.2). We now have

$$L_0 = (\mu x - y^2 + 2z^2 + \delta z)\frac{\partial}{\partial x} + (y(x-1))\frac{\partial}{\partial y} + (\mu z + \delta x - 2xz)\frac{\partial}{\partial z}, \tag{A.5}$$

$$L_2 = \epsilon\frac{\partial}{\partial y}, \tag{A.6}$$

and therefore

$$L_1 = \epsilon\left((x-1)\frac{\partial}{\partial y} - 2y\frac{\partial}{\partial x}\right), \tag{A.7}$$

$$L_3 = \epsilon\left[2\mu y\frac{\partial}{\partial x} + (-x^2 + (2+\mu)x - 1 + y^2 + 2z^2 - \delta z)\frac{\partial}{\partial y} + 2y(\delta - 2z)\frac{\partial}{\partial z}\right], \tag{A.8}$$

$$L_4 = -2\epsilon^2\frac{\partial}{\partial x}, \tag{A.9}$$

$$L_6 = \epsilon^2\left(2\mu\frac{\partial}{\partial x} + 2y\frac{\partial}{\partial y} + 2(\delta - 2z)\frac{\partial}{\partial z}\right). \tag{A.10}$$

These are elements of Σ_M for $M = 3$. For $(x, y, z = \delta/2)$ the operators in $\{L_1, L_2, L_3\}$ are linearly independent, while for $(x, y, z \neq \delta/2)$ $\{L_2, L_3, L_6\}$ are also linearly independent, which shows that the nondegeneracy condition is satisfied.

Appendix B. Boundedness

In this appendix we show that the attractor for the deterministic dynamics ($\epsilon = 0$) lies in a bounded region. This is done in a straightforward manner by using an approximate one-dimensional map for the successive minima of x given in [1]. There it is shown that the minimum value $x_{\min}$ achieved by x on the attractor depends on δ. For $\delta > 0$, $x_{\min}$ is bounded; for example, for $\delta \geq 0.2$, $x > -4$. Then the maximum $x_{\max}$ can be determined from the 1D map as $x_{\max} = -2 - x_{\min}$ for $x_{\min} < -2$. The results for $x_{\min}$ and $x_{\max}$ given in [1] are correct up to $O(\mu \ln \mu)$ for small μ. Therefore an $O(1)$ quantity could be added to the minimum and maximum values of x to give a slightly larger region in which the attractor is contained. Once the extreme values of x are known, the maximum values of y and z can also be determined.

We note that from the full system we have that $z > \delta/2$ and that y never crosses zero. Therefore we need to calculate only $y_{\max}$ and $z_{\max}$ to get bounds on the region of attraction. We will assume that y is initially positive, so that $y > 0$ for all time. By reflecting the dynamics across the plane $y = 0$ we can handle the case $y < 0$.

We describe briefly the derivation of the bounds for z and y. First we show that z is bounded by using the fact that $x_{\min} < x < x_{\max}$ where $x_{\min}$ and $x_{\max}$ are bounded for $\mu > 0$ and $\delta > 0$. This is done as follows.

$$\text{for } x > x_c(z) \equiv \frac{\mu z}{2(z - \delta/2)}, \quad \dot{z} < 0 \ (z \text{ approaches } \delta/2), \tag{B.1}$$

$$\text{for } x < x_c(z), \quad \dot{z} > 0, \tag{B.2}$$

$$\text{for } x > (<)1, \quad \dot{y} > (<)0. \tag{B.3}$$

Observations (B.1) and (B.2) indicate that z will be unbounded only if $x < x_c(z)$ for an infinitely long time. Suppose that $x < x_c(z)$. Then, observation (B.3) indicates that y decays (exponentially). Therefore y will eventually be negligible as compared to x and z. Therefore, the equations reduce to

$$\dot{x} = (\mu x + 2z^2 - \delta z)\,dt, \qquad \dot{z} = (\mu z + \delta x - 2xz), \tag{B.4}$$

$$\dot{y} = y(x - 1)\,dt. \tag{B.5}$$

Since $x < x_c(z)$, z increases, so that for z sufficiently large, $\dot{x} > 0$. In fact, x will continue to increase until $x > x_c(z)$. Then z decreases, approaching $\delta/2$. Therefore z must be bounded.

Since x and z are bounded, it is straightforward to show that y is bounded by introducing the quadratic function

$$V = x^2 + y^2 + z^2, \tag{B.6}$$

which, when following the dynamics of (1.2), changes by

$$\dot{V} = \mu(x^2 + z^2) - y^2. \tag{B.7}$$

This suggests that the dynamics are contracting for y sufficiently large, that is, when y is larger than $O(\mu)$. From (B.7) we also see why it is difficult to show that all orbits tend to a bounded set of zero volume using a simple Lyapunov function, as is done for the Lorenz system in [8,12]. A similar result can be obtained by using a quadratic function centered about the other unstable fixed point, $(1, \sqrt{\mu}, \delta/2 + O(\mu))$. In both cases we see that there is no contraction near the line $y = 0, z = \delta/2$.

Finally, we determine bounds on y and z. We have shown that for $x > 1$, y increases exponentially. In fact, y reaches its maximum for $x = 1$ and $y = O(1)$, which is the region termed Region 3 in Appendix C.3. There the dynamics are approximated by the semi-circle $(x-1)^2 + y^2 = K$, up to $O(\mu \log \mu)$ corrections, as shown also in [1], with $K = (x_{\max} - 1)^2 + O(\mu)$. Then $y_{\max}^2 = K + O(\mu \log \mu)$, so that an upper bound for y can be obtained by adding an $O(1)$ quantity to $x_{\max} - 1$.

To determine a bound for z, we consider the region in which $\dot{z} > 0$ (B.1) . As noted above, y is exponentially decreasing in this region, and the maximum value of z can be determined by looking at the reduced system considered in Section 8. Here the deterministic evolution is approximated by $x^2 + z^2 = C_4$, and (8.3). In matching this behavior to that of the dynamics considered in Appendix C, we find that $C_4 \sim x_{\min}^2 + \delta^2/4$, up to $O(\mu \ln \mu)$ corrections, as shown also in [1]. Then $z_{\max} \sim \sqrt{x_{\min}^2 + \delta^2/4}$. From this expression we get a bound on z.

When ϵ is positive then only the y variable is affected directly. The worst case is when the noise makes y stay close to zero, which results in large excursions in x and z. This happens with very low probability and, in fact, the random attractor is considerably smaller than the deterministic one, which is the main point of the paper.

Appendix C. The detailed expansion

We apply the approach outlined in the previous section to determine asymptotically $q_1(x, y)$ from (6.9). The stochastic system corresponding to (6.9) is

$$dx = (\mu G(x) - y^2)\,dt, \qquad dy = (y(x-1))\,dt + \sqrt{2}\epsilon\,dW. \tag{C.1}$$

For $\mu \ll 1$ the deterministic dynamics suggest three different scalings of x and y, as in [1]. We give an asymptotic approximation to $q_1(x, y)$ for each region. It is interesting to note that the scalings used for the local expansions of stationary solution of the Fokker–Planck equation are based on knowledge of the time-dependent dynamics. In Appendix D we use matched asymptotic expansions [16] to obtain a uniform approximation for the probability density.

C.1. Region 1: $(x-1) \ll \sqrt{\mu}$, $y \ll 1$

For the time-dependent dynamics, this region corresponds to slow time evolution of x with $y \ll 1$. This suggests that we scale y to be small, say, $\gamma v = y$ for $\gamma \ll \mu$. The appropriate scale γ depends on μ and ϵ, as shown in Appendix D. In fact, it is more direct to perform the calculations in terms of the original variables x and y, so we do not introduce the scaling explicitly in this section. With the assumption that $y \ll 1$ the leading order equations are

$$\dot{x} \sim \mu G(x), \qquad \dot{y} \sim y(x-1) + \sqrt{2}\epsilon\,dW. \tag{C.2}$$

To determine the leading order behavior $p_1(x, y)$ of $q_1(x, y)$ we use the approach described in Section 7. The deterministic motion is along the curves $y = F_1(x)$ where F_1 is determined by setting $\epsilon = 0$ in (C.2) and solving for y

$$y \sim F_1(x) \equiv \exp\left(\frac{1}{\mu}\left(\frac{1}{2}\log(x^2+\delta^2/4) - x + \delta/2\tan^{-1}(2x/\delta)\right) + C_1\right). \tag{C.3}$$

Then $p_1(x, y)$ denotes the leading order behavior of the density of the reduced problem in Region 1, where $p_1(x, y)$ is of the form (7.7) with

$$\begin{aligned} p_1 &\sim K(x)\exp\{-(y - F_1(x) - 2\epsilon/g_{1,n})^2 g_1(x)/2\epsilon^2)\}, \\ g_{1,n}(x) &= \exp\left(-\frac{2}{\mu}\int \frac{(x-1)}{x+\delta^2/4x}\,\mathrm{d}x\right), \\ g(x) &= \mu g_{1,n}(x)\Big/ 2\int \frac{1}{x'+\delta^2/4x'} g_{1,n}(x')\,\mathrm{d}x', \end{aligned} \tag{C.4}$$

$$K(x) = K_0 \exp\left(-\frac{1}{\mu}\int \frac{x-1}{x+\delta^2/4x}\,\mathrm{d}x\right)\Big/ (x+\delta^2/4x)\sqrt{g_{1,d}(x)}. \tag{C.5}$$

This approximation to the density is valid for small values of $x - 1$, as is shown by the matching in Appendix D.

In Region 1 the density is strongly peaked for y near $F_1(x)$ if $F_1(x) \gg \epsilon$, or $y = \mathrm{O}(\epsilon)$ if $F_1(x) \ll \epsilon$. The function $F_1(x)$ describes the deterministic dynamics, and involves a constant C_1. In Appendix D we show that the relative sizes of $\mathrm{e}^{(C_1-1)/\mu}$ and ϵ determine if the density is strongly peaked about the deterministic dynamics ($y = F_1(x)$) or if the noise dominates ($\epsilon \gg F_1(x)$).

C.2. *Region 2 ($x - 1 = \mathrm{O}(\mu^{1/2})$, $y = \mathrm{O}(\mu^{1/2})$)*

In Region 2, we use the scalings

$$y = \mu^{1/2}\eta, \qquad (x-1) = \mu^{1/2}\xi. \tag{C.6}$$

Following the same procedure as in Region 1, the leading order deterministic equations are

$$\dot{\xi} \sim \mu^{1/2}\left(1 + \frac{\delta^2}{4} - \eta^2\right), \qquad \dot{\eta} \sim \mu^{1/2}\eta\xi. \tag{C.7}$$

The solution curves have the form

$$\left(1 + \frac{\delta^2}{4}\right)\log\eta - \eta^2/2 + C_2 \sim \frac{\xi^2}{2}. \tag{C.8}$$

This does not give us an explicit function of $\eta = F_2(\xi)$. However, such a function is not necessary and we shall proceed as above. Then p_2, which is the leading order density for the reduced problem in Region 2, is of the form (7.7)

$$p_2(\xi, \eta) \sim K(\xi)\exp\{-(\eta - F_2(\xi) + 2\epsilon/\sqrt{g_{2,n}})^2 g_2(\xi)/2\epsilon^2)\},$$

with

$$g_{2,n}(\xi) = \frac{(1+\delta^2/4 - F_2^2(\xi))^2}{F_2^2(\xi)}, \qquad g_2(\xi) = \frac{g_{2,n}(\xi)}{2\int(1+\delta^2/4 - F_2^2(\xi'))/F_2^2(\xi')\,\mathrm{d}\xi'}, \tag{C.9}$$

$$K_2(\xi) = K_0 \frac{\exp(-2\int \xi'/(1+\delta^2/4 - F_2^2)\,\mathrm{d}\xi')}{\sqrt{g_{2,d}(\xi)}}. \tag{C.10}$$

C.3. Region 3 ($y = O(1)$)

In Region 3, both y and $x - 1$ are assumed to be O(1). Therefore we neglect the term μx, so that the leading order equations are

$$\dot{x} \sim -y^2, \qquad \dot{y} \sim y(x-1) + \sqrt{2}\epsilon \, dW. \tag{C.11}$$

The solution curves are given by

$$\frac{y^2}{2} \sim C_3 - \frac{(x-1)^2}{2} \equiv \frac{F_3^2(x)}{2}. \tag{C.12}$$

Then the leading order density of the reduced problem in Region 3 is given by $p_3(x, y)$ which is of the form (7.7) replaced by

$$p_3(x, y) \sim K(x) \exp\{-(y - F_3(x) - 2\epsilon/\sqrt{g_{3,n}})^2 g_3(x)/2\epsilon^2)\}, \tag{C.13}$$

with

$$g_{3,n}(x) = F_3^2(x), \qquad g_3(x) = -\frac{g_{3,n}(x)}{2(x-1) + D_3}, \qquad K_3(x) = \frac{K_0 F_3^2}{\sqrt{g_{3,d}(x)}}. \tag{C.14}$$

In the expression for $g_3(x)$ there is an arbitrary constant D_3 which will be determined by the matching.

Appendix D. The matching

As demonstrated in Figs. 1–3, for $\delta \ll 1$ the noise transforms the dynamics from chaotic to what we call noisily periodic behavior. In addition to yielding a uniform approximation to $q_1(x, y)$, the matching of the local expansions for it yields yields conditions under which we expect to see this striking effect. Therefore, we carry out the matching using an expansion about $\delta = 0$. The matching can also be done without such an expansion, but the analysis with this expansion is easier to follow.

We have found the behavior of the density in the three regions described above. In each region we have expanded about the deterministic dynamics, described by (C.3), (C.8), and (C.12). This expansion requires the determination of $F_j(x)$ in each region. In the definition of $F_j(x)$ there is an unspecified constant, denoted by C_j. We have proceeded with the expansion under the assumption that this constant can be determined. In fact, it is the matching of the local asymptotic expansions which fixes the constants. Therefore we can view the matched expansion as one about a "limit cycle" whose exact location is not determined until the matching is completed.

In order to match the local densities, we match the quadratic expressions in the exponents and the pre-exponential factors. We carry out the matching of the exponents between Regions 1 and 2. The matching between Regions 2 and 3 and the matching of pre-exponential factors goes exactly the same way.

The exponents from Regions 1 and 2 are

$$(y - F_1(x) + \epsilon/g_{1,n})^2 g_1(x)^2/(2\epsilon^2) \quad \text{for Region 1,} \tag{D.1}$$

$$(\eta - F_2(\xi) + \epsilon/(\mu^{1/2} g_{2,n}))^2 g_2(\xi)^2/(2\epsilon^2) \quad \text{in Region 2.} \tag{D.2}$$

As shown in (C.3) and (C.4), for $x - 1 \ll \mu^{1/2}$, $F_1(x) \sim e^{(C_1-1)/\mu}$ and $g_{1,n}(x) \sim 1$. In fact $F_1(1) = e^{(C_1-1)/\mu}$ gives the magnitude of y at $x = 1$ in the absence of noise. This is $y_{\min}$, the minimum value of y on the trajectory,

as noted in (3.2). Typically we write the exponent (D.1) in terms of a variable $y = \gamma(\mu, \epsilon)v$. This scaling depends on the relative magnitude of $e^{(C_1-1)/\mu}$ and ϵ, since it is appropriate to balance y with the maximum of either $F_1(x)$ or ϵ. We assume that $\epsilon \gg e^{(C_1-1)/\mu}$, and then determine conditions for the validity of this assumption.

Similarly, in Region 2 the exponent is written in terms of the appropriate scaled variables, η, and ξ, so that $\epsilon/\mu^{1/2}$ is negligible compared with $F_2(\xi)$, for $\epsilon \ll \mu$. That is, in Region 2, the deterministic behavior dominates the noise. Matching (D.2) to (D.1) corresponds to letting $\xi \to 0$. Then matching the dominant terms in these two exponents gives

$$\epsilon \sim \mu^{1/2} e^{-C_2}. \tag{D.3}$$

Here we have assumed that $e^{(C_1-1)/\mu} \ll \epsilon$, which we justify below. Then the constant C_1 does not play a role in the matching. The extreme values of x are found by considering the region in which they occur, that is, Region 2. As noted above in this region the deterministic motion dominates, so that the extreme values of ξ are gotten from the condition

$$\frac{d\xi}{d\eta} = 0. \tag{D.4}$$

From (C.8) we find that the maximum occurs for $\eta = 1$ and that $\eta(\xi_{\max})/\eta(\xi = 0) \sim \exp(-(x_{\max} - 1)^2/2\mu)$. Thus

$$(x_{\max} - 1)^2/\mu = -2C_2 + 1 = \left(1 - 2\log\frac{\epsilon}{\mu}\right). \tag{D.5}$$

In a similar manner, matching exponents from Regions 2 and 3 we obtain

$$\mu C_2 = C_3 + O(\epsilon). \tag{D.6}$$

In both of these regions the deterministic motion dominates, so that ϵ does not contribute to leading order in the matching. The matching gives the location of the curve about which the density is peaked. The graph of this curve is shown in Fig. 4.

We justify the assumption used above ($e^{(C_1-1)/\mu} \ll \epsilon$) by considering and eliminating the alternative, $e^{(C_1-1)/\mu} \gg \epsilon$. If this is the case, then we obtain $C_2 = (C_1 - 1)/\mu$ from the matching. Then F_2 can be used to determine the extreme value $x_{\max}$ in terms of C_1, as shown above. However, this leads to a value for $x_{\max}$ and a curve that disagree with the results of [2] and the simulations. For example, if $\epsilon = 10^{-7}$, then for $C_1 = 0.9$, $e^{(C_1-1)/\mu} \gg \epsilon$ and from the matching we find $x_{\max} \sim 1.4$, giving an orbit which is too small. In contrast, the simulations show that, in the chaotic regime, the deterministic motion follows the curve $y = F_1(x)$ which is an order of magnitude smaller than ϵ. Then relating C_1 to the deterministic values of $y_{\min}$ and $x_{\max}$ as in Section 3, $C_1 < 0.5$, and $e^{(C_1-1)/\mu} < 10^{-21}$. This is valid for a range of parameter values, for example, $\epsilon \geq 10^{-10}$ and $\mu = 0.01$. In [2] it is shown that the noisy periodicity replaces the chaotic behavior when $\mu|\ln\epsilon| \ll 1$. This is another way of expressing our assumption $e^{(C_1-1)/\mu} \ll \epsilon$ which we used in the matching.

As can be seen form the simulations, Fig. 3, the sharpness of the peak of the density is not uniform. Specifically, in Region 2 there is a transition from the sharply peaked behavior in Region 1, to a wider spread of the density in Region 3. Although this transition is not immediately obvious analytically, we show how this transition is captured by matching the local density approximations.

We now match the functions $g_j(x)$, whose definition includes an arbitrary constant. First we consider $g_2(\xi)$ in (C.9),

$$\begin{aligned} g_{2,n}(\xi) &= (1 - F_2^2(\xi))^2 \exp\left(-2\int \frac{\xi'}{1 - F_2^2(\xi')}\, d\xi'\right), \\ g_{2,d} &= \int \frac{-2g_{2,n}(\xi')}{1 - F_2(\xi')}\, d\xi'. \end{aligned} \tag{D.7}$$

Using the change of variables $\eta' = F_2(\xi')$, we write g_2 in terms of η

$$g_{2,n} = \frac{(1-\eta^2)^2}{\eta^2}, \qquad g_{2,d} = 2\int_{\eta_0}^{F_2(\xi)} \frac{-2(1-(\eta')^2)}{\eta'^3\sqrt{2\ln\eta' - \eta'^2 + 2C_2}}\,\mathrm{d}\eta'. \tag{D.8}$$

The constant η_0 was determined above by the matching of Regions 1 and 2, that is, $\eta_0 \sim \mathrm{e}^{-C_2}$. Let us rescale by $\eta' = \eta_0 z$ in $g_{2,d}$. Then

$$g_2 = \eta_0^2(1-\eta^2)^2 \Big/ 2\eta^2 \int_1^{F_2(\xi)/\eta_0} \frac{-2(1-\eta_0^2 z^2)}{z^3(2\ln z - \eta_0^2 z^2 + 2C_2)}\,\mathrm{d}z \tag{D.9}$$

so that as η varies from $\mathrm{O}(\eta_0)$ to $\mathrm{O}(1)$ values, g_2 varies from $\mathrm{O}(1)$ to $\mathrm{O}(\eta_0^2) = \mathrm{O}(\epsilon^2/\mu)$. The change in behavior of g_2 comes from the change in the behavior of the density in Region 2. For small values of y (and η) the density matches to the behavior in Region 1, where the density is strongly peaked as implied by the $\mathrm{O}(\epsilon^2)$ scaling in the exponent in (7.7), with g given by (C.4). For $\mathrm{O}(1)$ values of η, the width of the density increases. So we must match with Region 3. Writing g_3 in terms of ξ and η to match (C.14) with (D.9) gives

$$D_3 \sim \left\{ 2\int_1^{\infty} \frac{-2(1-\eta_0^2 z^2)}{z^3(2\ln z - \eta_0^2 z^2 + 2C_2)}\,\mathrm{d}z \right\} \Big/ \eta_0^2 = \mathrm{O}(\mu\epsilon^{-2}). \tag{D.10}$$

The peak of the density in Region 3 is, therefore, given by the $\mathrm{O}(\mu)$ scaling. This matching of g_2 with g_1 and g_3 describes how the shape of the density goes from sharply peaked in Region 1 to a wider spread in Region 3, as can be seen from the simulations in Fig. 3. The contour plot of the matched density is shown in Fig. 5.

References

[1] Hughes, M.R.E. Proctor, Chaos and the effect of noise in a model of three-wave mode coupling, Physica D 46 (1990) 163–176.
[2] G.D. Lythe, M.R.E. Proctor, Noise and slow-fast dynamics in a three wave resonance problem, Phys. Rev. E 47 (1993) 3122–3127.
[3] Y. Kifer, Computations in dynamical systems via random perturbations, Discr. and Cont. Dynam. Sys. 3 (1997) 457–476.
[4] M.I. Friedlin, A.D. Wentzell, Random Perturbations of Dynamical Systems, Springer, Berlin, 1984.
[5] Z. Schuss, Theory and Applications of Stochastic Differential Equations, Wiley, New York, 1980.
[6] T. Naeh, M.M. Klosek, B.J. Matkowsky, Z. Schuss, A direct approach to the exit problem, SIAM J. Appl. Math. 50 (1990) 595–627.
[7] B. White, The effects of a rapidly-fluctuating random environment on systems of interacting species, SIAM J. Appl. Math. 32 (1977) 666–693.
[8] Y. Kifer, Random Perturbations of Dynamical Systems, Birkhäuser, Boston, Basel 1988.
[9] H. Keller, Attractors and bifurcations of the stochastic Lorenz system, Universität Bremen, Institute für Dynamische Systeme, Report 389, 1996.
[10] C. Sparrow, The Lorenz Equations: Bifurcations, Chaos, and Strange Attractors, Springer, New York, 1982.
[11] L.A. Bunimovich, Ya.G. Sinai, Stochasticity of the attractor in the Lorenz model, in: A.V. Gaponov-Grekhov (Ed.), Nonlinear Waves, Nauka, Moskow, 1979, pp. 212–226.
[12] L.A. Bunimovich, Statistical properties of Lorenz attractors, in: G.I. Barenblatt et al. (Eds.), Nonlinear Dynamics and Turbulence, Pitman, Boston, 1983, pp. 71–92.
[13] D. Nualart, The Malliavin Calculus and Related Topics, Springer, Berlin, 1995.
[14] R.S. Maier, D.L. Stein, Limiting exit location distributions in the stochastic exit problem, SIAM J. Appl Math. 57 (1997) 752–790.
[15] R.S. Maier, D.L. Stein, Oscillatory behavior of the rate of escape through an unstable limit cycle, Phys. Rev. Lett. 77 (1996) 4860–4863.
[16] C. Bender, S. Orszag, Advanced Mathematical Methods for Scientists and Engineers, McGraw-Hill, New York, 1978.
[17] G.D. Lythe, Dynamics controlled by additive noise, in: Fluctuations in Physics and Biology: Stochastic Resonance, Signal Processing and Related Phenomena, Nuovo Cimento D, vol. 170, 1995.
[18] S. Baer, R. Kuske, Probability densities for noisy delay bifurcations, in preparation.